Interactions of 3T3 fibroblasts and endothelial cells with defined pore features

A. K. Salem,[1] R. Stevens,[2] R. G. Pearson,[1] M. C. Davies,[1] S. J. B. Tendler,[1] C. J. Roberts,[1] P. M. Williams,[1] K. M. Shakesheff[1]

[1]*School of Pharmaceutical Sciences, University of Nottingham, Nottingham, NG7 2RD, United Kingdom*
[2]*Central Microstructure Facility, Rutherford Appleton Laboratory, Chilton, Didcot, Oxfordshire OX11 0QX, United Kingdom*

Received 6 June 2001; revised 27 November 2001; accepted 12 December 2001

Abstract: The colonization of biodegradable polymer scaffolds with cell populations has been established as the foundation for the engineering of a number of tissues, including cartilage, liver, and bone. Within these scaffolds, the cells encounter a porous environment in which they must migrate across the convoluted polymer surface to generate a homogenous cell distribution. Predicting the interactions between cells and pores is important if scaffold characteristics are to be optimized. Therefore, we investigated the behavior of two model cell types over a range of defined pore features. These pore features range from 5 to 90 μm in diameter and have been fabricated by photolithographic techniques. Quantitatively, the behavior of the cells is dependent on three factors: 1) percentage cell coverage of the surface; 2) pore size; and 3) cell type. Fibroblast cells displayed a cooperative pattern of cell spreading in which pores with diameters greater than the cell dimensions were bridged by groups of cells using their neighbors as supports. Endothelial cells were unable to use neighbors as support structures and failed to bridge pores greater than the cell diameter. © 2002 Wiley Periodicals, Inc. J Biomed Mater Res 61: 212–217, 2002

Key words: tissue engineering; 3T3 fibroblasts; endothelial cells; porosity; photolithography

INTRODUCTION

The use of biodegradable polymer scaffolds as templates for tissue engineering has been described for a number of tissue types, including cartilage, liver, and nervous tissue.[1–4] Within these scaffolds, the seeded cells encounter a high surface area formed by the polymer. This surface is convoluted to form a three-dimensional structure containing many pores.[5–8] The success of the tissue engineering is dependent on the migration of cells through this porous environment and the maintenance of nutrient diffusion throughout the scaffold after cell colonization. Ideally, after seeding, the cell population should be able to migrate through the scaffold and some pores should remain open to allow nutrient diffusion as the tissue forms.

To study the effect of pore diameter on cell migration and morphology, we used nanofabrication to form surfaces with defined porosities, enabling the study of cell behavior over these defined topographical features. Two cell types have been chosen for these studies: 3T3 fibroblasts and bovine aortic endothelial cells. Cell type choice was made as a result of the different behavior of these cells during tissue formation *in vivo*. Fibroblasts tend to fill spaces within tissues and form extracellular matrix, whereas endothelial cells form into tubular architectures in which the integrity of a central lumen is essential to blood vessel function.

It has been widely reported that a change in surface topography can influence cell behavior substantially. Micron-scale roughness has been shown to modify cellular responses in cell culture and to modify biocompatibility and tissue attachment significantly.[9] Cell spreading and cell shape, and their effects on cell growth and cell function, have also been shown to be dependent on surface morphology.[10,11] One theory is that topography affects cell behavior by altering the ability of the extra-cellular matrix (ECM) to absorb to the surface.[9,12] Topographical features have been shown to orient cells in a phenomenon known as "contact guidance".[12–19] It has been suggested that features that involve a change in the direction from one

Correspondence to: K. M. Shakesheff; e-mail: kevin.shakesheff@nottingham.ac.uk

surface configuration into another as produced by hills, pits, grooves, or edges extending out into the main plane or an edge where two planes meet may be seen as discontinuities.[9] Cells attach to a surface by a number of contacts, including podosomes, point contacts, and focal contacts.[12] These focal adhesions consist of a cluster of ECM-bound integrins that act as a membrane attachment for the actin fibrils inside a cell.[20,21] There is a great deal of evidence to suggest that there is a concentration of these focal adhesion points at discontinuities.[14,17,22,23] Intracellular proteins involved in the focal adhesions crosslink the actin microfilaments, whose structure determines cell shape maintenance.[9] Integrins link the external ECM to the intracellular actin cytoskeleton, and it is the presence of the concentrated actin at the discontinuities as detected by phalloidin staining that confirms the theory of focal adhesion points being formed at discontinuities.[9,13,17,20–23]

There are a number of factors involved in the behavior of cells over topographical features.[16] Cell density has been shown to have a significant role in the behavior of cells over a defined surface. When BHK (fibroblastic) cells were compared directly to MDCK (epithelial) cells, MDCK cells in co-culture were often unaffected by topographical features that would strongly orientate single MDCK and BHK cells.[23] Where topographical features are on the nanometre scale, cell-cell interactions have in fact been found to be the more dominant factor in determining cell guidance.[15] There are also clear differences in behavior between different cell types.[16,17] This may be attributed to different amounts of actin monomer available in different cell types. A cell with less actin monomer will use the majority of this in forming a polymer once in contact with a discontinuity, thus reducing further movement or spreading of the cell and limiting its movement to around the discontinuity.[23] Some cell types may display co-operative behavior with topographical features. This has been demonstrated when cells migrating along fibers attached to other cells to form "sail sheets" to get from one topographical feature to another where the depth was too great.[23]

MATERIALS AND METHODS

Silicon nitride template manufacture

Porous silicon nitride membranes were manufactured using a multistage process (Fig. 1). Double-sided polished silicon wafers 300-microns thick were cleaned and coated with low-stress silicon nitride using low-pressure chemical vapor deposition. The surface topography design was written to an electron beam pattern generator (Ebeam) and then transferred to two chrome masks to define the back-etch mask and the pore size and layout. Silicon wafers coated on both sides with silicon nitride were dehydrated at 150°C for 30 min. On cooling, these were coated with hexamethyldisilizane as an adhesion promoter. The back-etching of the wafer was achieved as follows. One side of the wafer was spin coated with 250 μL of photoresist (AZ5214E) for 60 s at 3000 rpm. After a solvent bake at 100°C for 90 s, the wafer was exposed to UV light from a mercury vapor lamp. The exposure energy was 100 $mJcm^{-2}$. The exposed resist was developed in a 4:1 mixture of de-ionized water: AZ-400K developer, rinsed with de-ionized water and then spun dry with a nitrogen purge. The substrate was then hard-baked for 30 min at 120°C. An oxygen plasma descum was used to re-

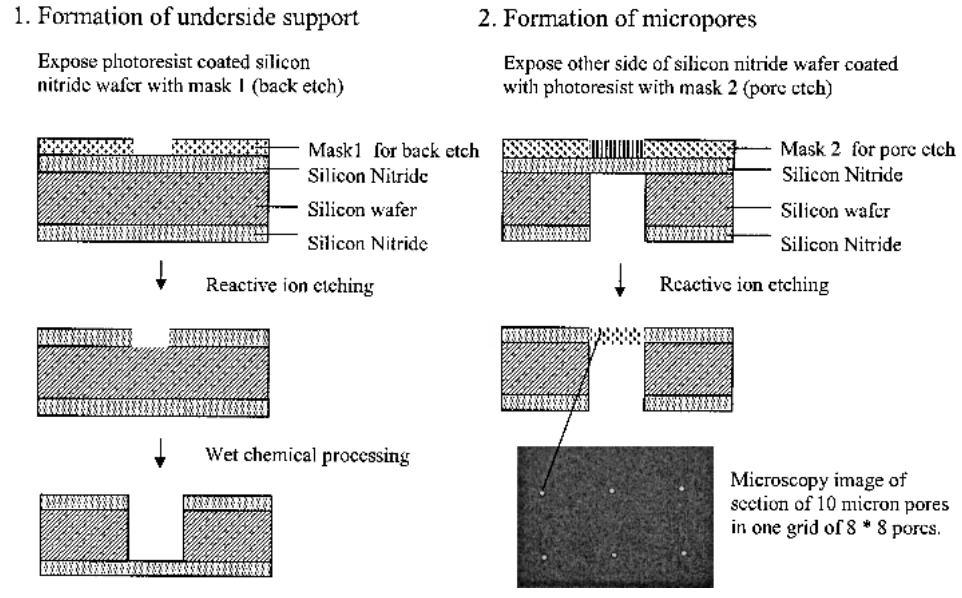

Figure 1. Schematic of pore template manufacture.

move organic residues from the exposed nitride surface. The oxygen plasma was achieved with a flow rate of 35 standard cubic centimetres (SCCM) of electronic grade oxygen, a process pressure of 200 mTorr, and a radio frequency plasma power of 100 watts at 13.65 MHz for a duration of 0.7 min. Reactive ion etching of the silicon nitride was performed in a fluorine-based plasma. The process conditions were 35 SCCM of CHF_3, 5 SCCM of O_2 at a pressure of 100 mTorr, and power of 150 watts for 15 min. An oxygen plasma resist strip at 35 SCCM O_2 (200 millitores, 100 watts) for 15 min ensured that surface chemistry and topography would be the same and this was confirmed by a Tencor P2 long scan profiler. After cleaning and drying in nitrogen, the substrate was back etched using 45% potassium hydroxide (KOH) in de-ionized water. To etch the pores onto the silicon nitride wafer, the back-etched substrates were coated with a hexamethyldisilizane adhesion promoter at 150°C and then coated with photoresist (AZ5214E). The substrate was then exposed to UV light under the mask with the pore designs. Reactive ion etching and plasma cleaning were performed under identical conditions, but on the other side of the wafer. Once the pores were defined the wafer was cleaned using a photoresist stripper (1-amino-propan-2-ol, AZ-100 remover), rinsed in deionised water, and then dried.

Cell culture

3T3 fibroblasts (ATCC) and bovine aortic endothelial cells (ECACC) were cultured in DMEM supplemented with 10% fetal calf serum, 2 m*M* L-glutamine, 100 U/mL penicillin, 100 μg/mL streptomycin and 0.25 μg/mL amphotericin B. Cell cultures were incubated at 37°C in a 5% CO_2-enriched atmosphere. Silicon nitride substrates were coated for 24 h with 10 mg/mL fibronectin dissolved in de-ionized water. Substrates were washed three times with de-ionized water before seeding with cells. A cell seeding density of 7000 cells/cm^2 was used in all studies.

For phalloidin staining of cytoplasmic actin filaments. Cells were fixed in 2% glutaraldehyde for 24 h, washed with phosphate buffered saline. 0.1% Triton-X was added for 10 min, removed and washed. Phalloidin (250 μg/mL) in phosphate-buffered saline was then incubated with cells for 30 min. The samples were washed several times in phosphate-buffered saline.

Microscopy and time-lapse studies

Phase contrast images were taken on an optical microscope (Leica DMIRB) attached to a Leica Q500 IW using a colour video camera (JVC TK-C1380). Time-lapse studies were captured on the optical microscope in an environmental chamber (Leica) at 37.1°C (Solent Scientific Incubator Temperature) in a 5% CO_2-enriched environment (Linkam CO 102). Images were taken every 10 min over 24- to 48-h periods. Cell coverage calculations were made using Leica Qwin Software.

Quantification

Each set of pores, of a defined size, are set in an 8 by 8 array in a window of 3.2 mm by 3.2 mm. Each pore was separated by 320 μm in both the x- and y-axis. Measurements were taken on every pore within a window at set intervals of 4, 24, 48, and 72 h. Further measurements were made every 24 h as necessary. Statistical analysis of the cell behavior was calculated using one-way analysis of variance (ANOVA) with a Tukey post-test for the purposes of comparing pairs of group means, from data at each time point.

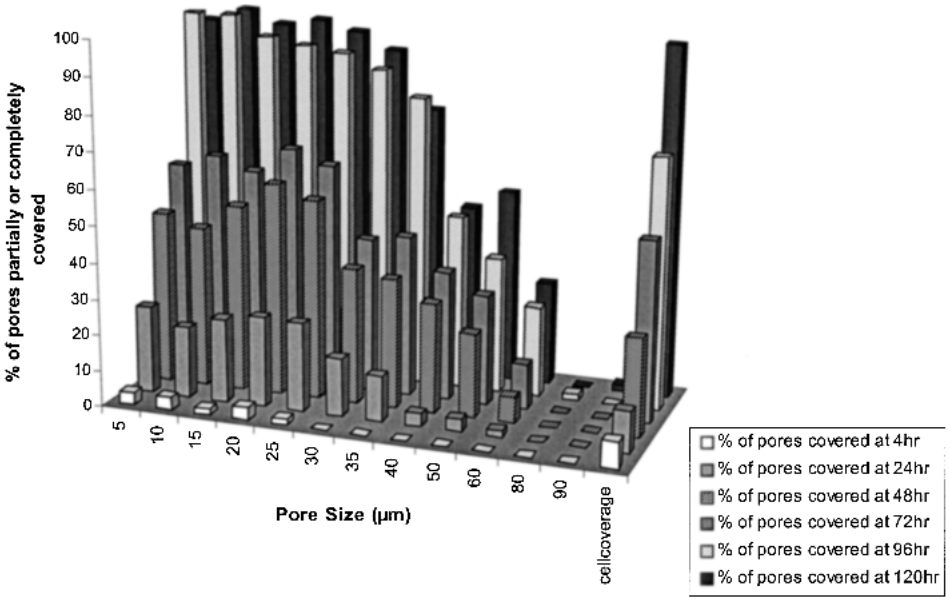

Figure 2. Bar graph showing percentage pore coverage with endothelial cells over a 120-h period.

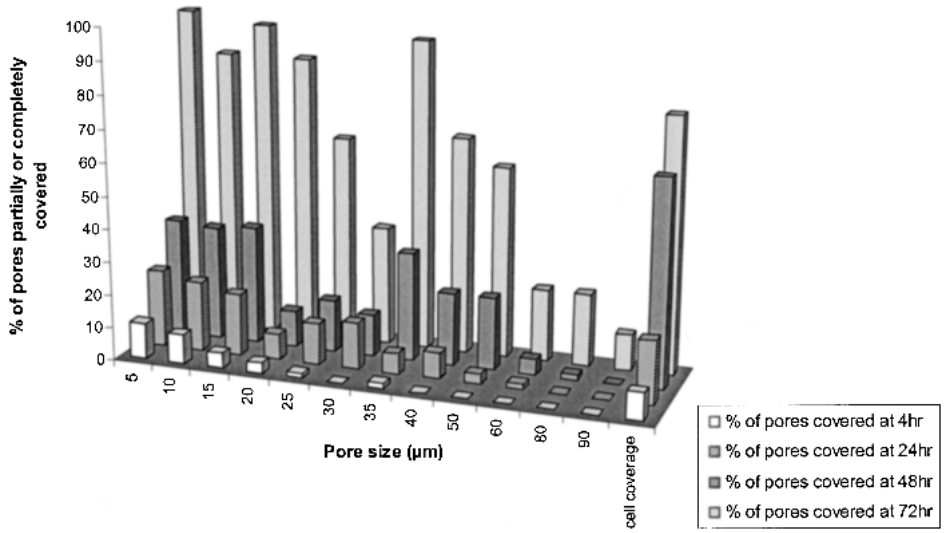

Figure 3. Bar graph showing percentage pore coverage with 3T3 fibroblasts over a 72-h period.

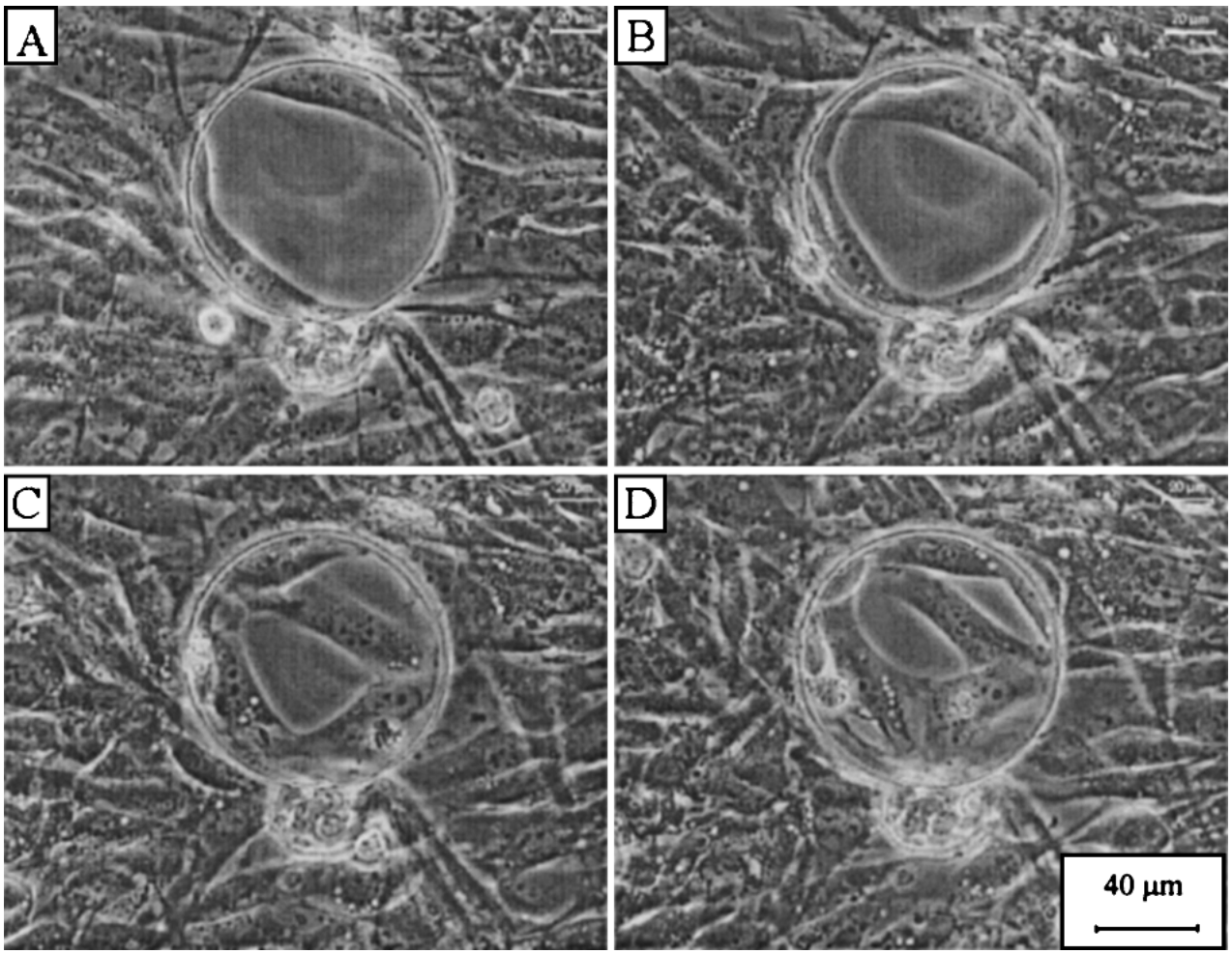

Figure 4. Fibroblasts displaying co-operative behavior at confluence to cross a 100-µm pore over a 6-h period. (A) 0 h; (B) 2.5 h; (C) 5.0 h; (D) 6 h.

RESULTS AND DISCUSSION

Endothelial cells

The endothelial cell population reached maximum cell coverage of the silicon substrate after 120 h of culturing on the samples. As shown in Figure 2, the endothelial cells did not cover any part of a pore of 80 or 90 μm in diameter at any time point. Even at the 120-h point, when the rest of surface was essentially entirely covered, the 80- and 90-μm pores were entirely uncovered.

As the pore diameter was decreased from 60 to 30 μm, the number of pores that were partially or completely covered by an endothelial cell increased. Considering the 30-μm pores, the probability that a pore was covered or partially covered was related directly to the total pore coverage ($p > 0.05$; Fig. 2). In comparison, the extent of pore coverage for 40-, 50-, and 60-μm pore diameters was lower than the overall substrate cell coverage ($p < 0.05$). At pore diameters of less than 30 μm, the endothelial cells were able to cover the pores to the same extent as the rest of the silicon substrate ($p > 0.05$).

Overall, it can be concluded that for endothelial cells on this substrate, the cells cannot cover pores of 80 μm or more diameter, they are unaffected by pores of 30 μm or less, and that a linear relationship exists between cell coverage and pore size between 30 μm and 80 μm.

3T3 fibroblasts

This cell type displayed a more complex pattern of interaction with the pores than the endothelial cells. The results for 3T3 fibroblasts/pore interactions are shown in Figure 3. Here, the fibroblasts reached maximum cell coverage of the silicon substrate after 72 h of culture. The percentage of pores covered at 48 h in comparison to the percentage of pores covered at 72 h was considered extremely significant ($p < 0.001$). Up to and including the time point at 48 h, the fibroblasts were unable to cover or partially cover the 80- and 90-μm pores. However, at 72 h, between 20 and 30% of these larger pores became covered. Beyond 72 h, all pores were covered by the confluent fibroblasts.

For the other pores sizes, any trend in fibroblast coverage is less apparent, in comparison with the endothelial cells, and fibroblast coverage was found to be more variable. However, in general, fibroblasts were able to cover pores of 50 μm and less.

Given the fact that the spread 3T3 fibroblasts (20 to 50 μm diameter) are significantly smaller than the endothelial cells (60 to 200 μm diameter), the ability of the smaller cell type to cover larger pores indicates a difference in the nature of interaction between the two cell types and pores. The mechanism by which fibroblasts can bridge the large pores is shown in Figure 4, where time-lapse images show confluent 3T3 fibro-

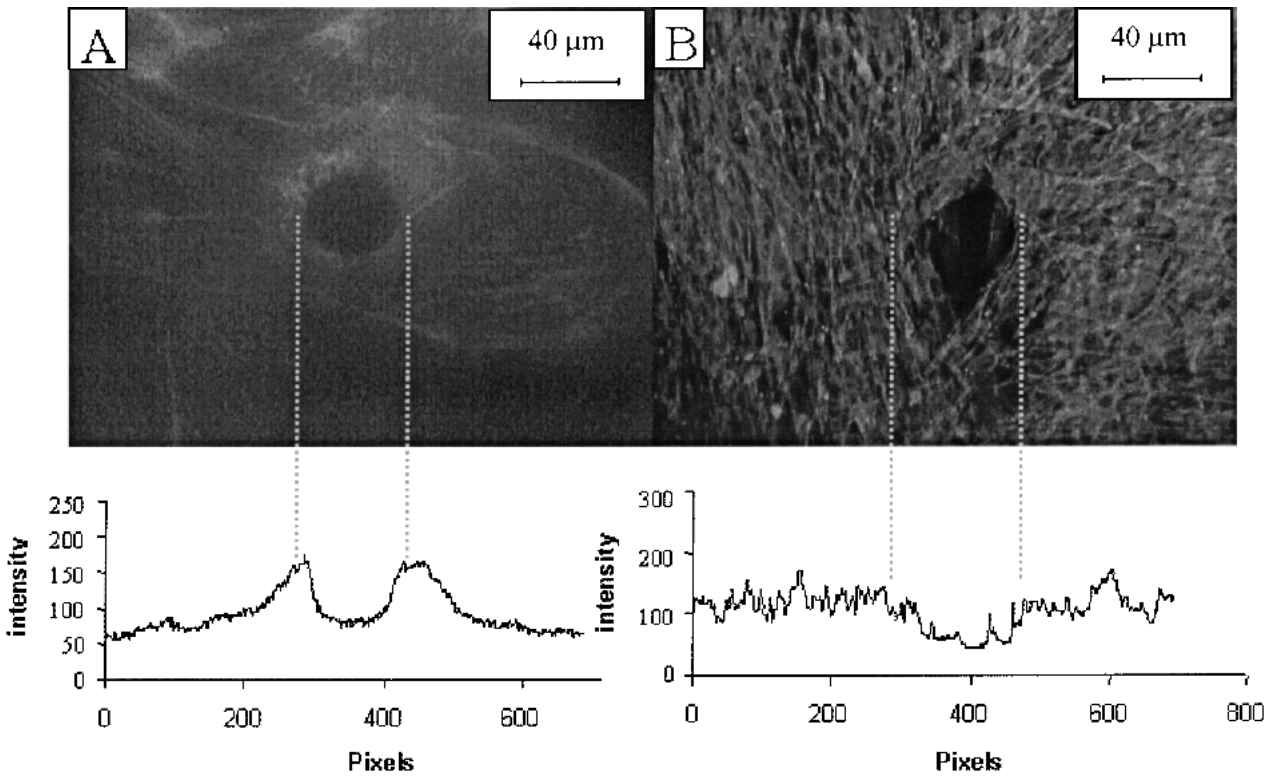

Figure 5. Phalloidin stained images with analysis of cross-section to show cytoskeletal distribution of actin at the topographical features with (A) endothelial cells over a 40-μm pore and (B) 3T3 fibroblasts around a 50-μm pore.

blasts use neighbors as supports to cross pore features larger than the individual fibroblast dimensions. The idea of cells responding to the pores as a topographical discontinuity, are consistent with the findings of Curtis et al., who demonstrated that cells migrating along fibers would often attach laterally to cells already on the fibers or at bends to form "sail sheets" to cross to another topographical feature, where the depth was too great to overcome.[23]

The difference in the behavior of the two cell types can be further highlighted through phalloidin staining, which confirms that the cells are responding to the pores as topographical discontinuities. Fluorescence microscopy images in Figure 5 show the two cell types around the pores, which were fixed with glutaraldehyde and stained with phalloidin. Light intensity cross-sections of the images revealed the lateral variations in the cytoskeletal distribution of each cell type. The cytoskeleton in the endothelial cells [Fig. 5(a)] is limited by the boundary of the pore with concentrated regions of cross-linked actin around the edge of the topographical feature. In contrasts, the distribution of cytoskeleton in fibroblasts [Fig. 5(b)] is unchanged by the pore boundary. Thus, the cells ability to cover pores may be reflected by the actin assembly occurring within the cells. With the endothelial cells, the actin assembly occurs predominantly at the pore edge. This results in concentrated focal adhesion contacts at the pore edge limiting further movement. The fibroblasts also form significant focal contacts; however, these are not restricted to the pore edge. As a result, the fibroblasts are able to orientate around the pore features and display greater mobility. They may cross the boundary of the pore and then use their neighboring cells as support structures.

CONCLUSION

Porosity has been shown to influence the behavior of cells. This study of cells over defined pore features has determined that cell behavior is interlinked by three factors: 1) cell type; 2) pore size; and 3) cell density. It has also been shown that the cells respond to the pores as topographical discontinuities. The difference in behavior of the two cell types is related to the cytoskeletal structure and actin monomer content. However, in both cell types, cell density and pore size affected percentage pore coverage significantly. These results confirm that within a tissue, engineering scaffold cells displaying fibroblast behavior will tend to block pores even where the pore diameter is greater then the cell diameter.

A.K. Salem thanks EPSRC for funding. AKS thanks S. Dexter for assistance in cell culturing techniques and G.R. Thomas for assistance in training in photolithographic techniques.

References

1. Hutmacher DW. Scaffolds in tissue engineering bone and cartilage. Biomaterials. 2000;21:2529–2543.
2. Bellamkonda R, Aebischer P. Review: Tissue engineering in the nervous system. Biotechnol Bioeng 1994;43:543–554.
3. Baldwin SP, Saltzman WM. Polymers for tissue engineering. Trends Polymer Sci 1996;4:177–182.
4. Den Dunnen WFA, Van Der Lei B, Schakenraad JM, Blaauw EH, Stokroos I, Pennings AJ, Robinson PH. Long-term evaluation of nerve regeneration in a biodegradable nerve guide. Microsurgery 1993;14:508–515.
5. Athanasiou KA, Schmitz JP, Agrawal CM. The effects of porosity on in vitro degradation of polylactic acid polyglycolic acid implants used in repair of articular cartilage. Tissue Engineering 1998;4:53–63.
6. Evans GRD, Brandt K, Widmer MS, Lu L, Meszlenyi RK, Gupta PK, Mikos AG, Hodges J, Williams J, Gurlek A, Nabawi A, Lohman R, Patrick CW. In vivo evaluation of poly(L-lactic acid) porous conduits for peripheral nerve regeneration. Biomaterials 1999;20:1109–1115.
7. Wake MC, Patrick CW, Mikos AG. Pore morphology effects on the fibrovascular tissue growth in porous polymer substrates. Cell Transplatation 1994;3:339–343.
8. Kaufmann PM, Heimrath S, Kim BS, Mooney DJ. Highly porous polymer matrices as a three-dimensional culture system for hepatocytes. Cell Transplantation 1997;6:463–468.
9. Von recum AF, Van kooten TG. The influence of microtopography on cellular-response and the implications for silicone implants. J Biomater Sci-Polym 1995;7:181–198.
10. Singhvi R, Stephanopoulos GN, Wang DIC. Effects of substratum morphology on cell physiology - review. Biotechnol Bioeng 1994;43:764–771.
11. Singhvi R, Kumar A, Lopez GP, Stephanopoulos, GN, Wang DIC, Whitesides GM, Ingber D E. Engineering cell-shape and function. Science 1994;264:696–698.
12. Meyle J, Gultig K, Brich M, Hammerle H, Nisch W. Contact guidance of fibroblasts on biomaterial surfaces. J Mater Sci-Mater Med 1994;5:463–466.
13. Brunette DM. Spreading and orientation of epithelial-cells on grooved substrata. Exp Cell Res 1986;167:203–217.
14. Brunette DM. Fibroblasts on micromachined substrata orient hierarchically to grooves of different dimensions. Exp Cell Res 1986;164:11–26.
15. Clark P, Connolly P, Curtis ASG, Dow JAT, Wilkinson CDW. Cell guidance by ultrafine topography in vitro. J Cell Sci 1991; 99:73–77.
16. Clark P. Cell behaviour on micropatterned surfaces. Biosensors Bioelectronics 1994;9:657–661.
17. Flemming RG, Murphy CJ, Abrams GA, Goodman SL, Nealey PF. Effects of synthetic micro- and nano-structured surfaces on cell behavior. Biomaterials 1999;20:573–588.
18. Curtis ASG. Nanofabrication and its applications in medicine and biology. Eng Phys Proc 1994;Chapter 3:41–55.
19. Den braber ET, Deruijter JE, Smits HT.J, Ginsel LA, Von recum AF, Jansen JA. Effect of parallel surface microgrooves and surface-energy on cell-growth. J Biomed Mater Res 1995;29:511–518.
20. Ruoslahti E. Cell biology—Stretching is good for a cell. Science 1997;276:1345–1346.
21. Ruoslahti E, Obrink B. Common principles in cell adhesion. Exp Cell Res 1996;227:1–11.
22. Curtis A, Wilkinson C. Topographical control of cells. Biomaterials 1997;18:1573–1583.
23. Curtis ASG, Clark P. The effects of topographic and mechanical-properties of materials on cell behavior. Crit Rev Biocompatibil 1990;5:343–362.